Characterization of Adult Onset Lamin B1 Depletion in an Inducible Knockout Mouse Model

by

Anushe Munir

BS Applied Biosciences, National University of Sciences and Technology, 2017

Submitted to the Graduate Faculty of the

Department of Human Genetics

Graduate School of Public Health in partial fulfillment

of the requirements for the degree of

Master of Science

University of Pittsburgh

2020

UNIVERSITY OF PITTSBURGH

GRADUATE SCHOOL OF PUBLIC HEALTH

This thesis was presented

by

Anushe Munir

It was defended on

June 11, 2020

and approved by

Robert D. Nicholls, DPhil Professor of Pediatrics, School of Medicine, University of Pittsburgh

Zsolt Urban, PhD, Associate Professor of Human Genetics, Graduate School of Public Health, University of Pittsburgh

Thesis Advisor: Quasar S. Padiath, MBBS, PhD, Associate Professor of Human Genetics, Graduate School of Public Health, University of Pittsburgh

Quasar S. Padiath, MBBS, PhD,

**Characterization of Adult Onset Lamin B1 Depletion in an Inducible
Knockout Mouse Model**

Anushe Munir, MS

University of Pittsburgh, 2020

Abstract

Autosomal dominant leukodystrophy (ADLD) is a rare, adult onset neurological disorder. It is a type of leukodystrophy that initially presents with autonomic dysfunction leading to cerebellar and pyramidal abnormalities as the disease progresses. ADLD is caused by an overexpression of *LMNB1* located on chromosome 5q23.2. Currently numerous potential therapies are being investigated where the aim is to reduce this gene's overexpression in an attempt to manage the symptoms. However, previous research carried out using knockout mouse models has established *Lmnb1* as a critical component essential during development. Studies focusing on total *Lmnb1* knockout mice recorded postnatal lethality due to multiple pathologies impacting organ development and severe abnormalities in skeletal structure. The public health significance of our study lies in how we aim to explore the effects of *Lmnb1* reduction in adulthood as a precursor to developing effective therapies for ADLD. We demonstrate how the ablation of *Lmnb1* in adult mice impacts their phenotype; behavior and overall molecular makeup, in an attempt to observe any deleterious effects that may arise. Using a tamoxifen inducible Cre*/Lox*P system, we created conditional knockout mice where the *Lmnb1* gene was targeted for deletion only in adulthood. After collecting, quantifying and studying our behavioral, molecular, and immunofluorescence data we were able to demonstrate that reduced *Lmnb1* expression in adulthood produced no obvious pathological alterations.

Table of Contents

List of Abbreviations

ADLD	Autosomal Dominant Leukodystrophy
ACTB	Beta Actin
cKO	Conditional Knockout
CNS	Central Nervous System
Ctrl	Control mouse cohort
DMEM	Dulbecco's Minimal Essential Medium
DPBS	Dulbecco's phosphate-buffered saline
Fb	Forebrain
Flox or fl/fl	Flanked by *LoxP* sequences
Hrt	Heart
Htt	Mouse gene for huntingtin protein
IHC	Immunohistochemistry
IP	Intraperitoneal
Lb1	Lamin B1
LD	Leukodystrophy
Liv	Liver
Lmnb1	Mouse gene for lamin b1 protein
LMNB1	Human gene for lamin b1 protein
LMNB1	Lamin B1 protein
MS	Multiple Sclerosis
PBS	Phosphate buffered saline
PNS	Peripheral Nervous System
PPC	Preclinical Phenotyping Core
RPM	Rotations per Minute
Sc	Spinal cord
TUBB4A	Tubulin housekeeping gene
UBC Cre	Ubiquitous Cre
Wt	Wild type

List of Tables

List of Figures

Preface

      I would like to begin by saying thank you to Dr. Quasar Padiath for taking me into his Lab and being a great mentor for my master's thesis project. With his encouragement and positive reinforcement, I was able to learn so many new techniques and concepts all of which will continue to help me as I progress in my scientific career. I also want to say a big thank you to everyone in the Padiath Lab; Fang, Talia, Guillermo, Virali. Specifically, Bruce and Nathan, for taking out time whenever I needed and for going out of their way to help me with the smallest of my concerns. A big thank you to Dr. Zsolt Urban and Dr. Rob Nicholls for their guidance, feedback and for being a part of both my comprehensive exam and thesis defense committees.

      I also want to thank my family; Mama and Papa, I would not have been able to do this without your prayers, constant support and all those facetime phone calls to keep me going, my fiancé – Sameed, for being a constant source of comfort and encouragement during this entire experience.

      Lastly, I want to acknowledge everyone at the Department of Human Genetics, every faculty member, administrative aid and student has helped me in many ways and made my time away from home in the US very memorable.

1.0 Introduction

1.1 Autosomal Dominant Leukodystrophy (ADLD)

Myelin, a critical component of all vertebrate nervous systems, is synthesized by oligodendrocytes in the central nervous system (CNS) and Schwann cells in the peripheral nervous system (PNS). It is an insulating layer that encapsulates and protects axons and is responsible for facilitating the rapid transmission of nerve impulses [1] (**figure 1**). Demyelination or the loss of myelin can occur either as a primary pathology or secondary to other diseases that affect the CNS and PNS. Leukodystrophies (LD) are a large group of highly heterogeneous, inherited diseases involving the CNS that primarily impact myelin. They are distinct from multiple sclerosis (MS) as they are usually caused by mutations in single genes with each gene defect translating into a different type of LD [2]. One such leukodystrophy is Autosomal Dominant Leukodystrophy (ADLD).
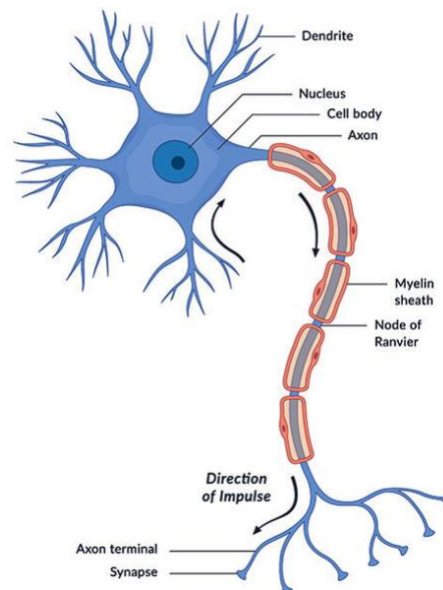
Figure 1: Neuron Illustration

Figure 1: Simple diagrammatic representation of a neuron showing the how the myelin sheath encapsulates the axons aiding in nerve impulse transmission. (Image source: US National Institutes of Health https://www.nichd.nih.gov/health/topics/neuro/conditioninfo/parts)

ADLD is a rare adult onset neurological disorder manifesting in the fourth or fifth decade of life [3]. The exact prevalence rate is unknown, however documented cases have been observed in families from around the world with various ethnic origins; French-Canadian [4], Japanese [5], Italian [6]. It initially presents with autonomic dysfunction with symptoms that include loss of bladder control, erectile dysfunction, postural hypotension and constipation [7]. Further disease progression can result in increased complications including cerebellar and pyramidal abnormalities (weakness and spasticity observed in upper and lower extremities), with some severe cases also developing cognitive dysfunction during the advanced stage. In the early stages it can be difficult to diagnose ADLD with the possible differential diagnosis being other leukodystrophies that have an adult onset or multiple sclerosis (MS) and Vitamin B12 deficiencies [7]. For a definitive diagnosis a Magnetic Resonance Imaging (MRI) is carried out, where specific brain and spinal cord demyelination patterns are used as the indication of ADLD [8].

1.2 Molecular Mechanism

ADLD is caused by the duplication of the lamin b1 gene (*LMNB1*) on chr 5q23.2 [5]. Tissue analysis of normal and ADLD samples confirmed increased LMNB1 expression levels in the affected individuals compared to the controls [5]. The LMNB1 protein is a type of intermediate filament protein which, with other lamin proteins, works to provide structural support to the nuclear envelope. The lamin proteins, lamin A/C and lamin B1/B2, also play a significant role in

gene expression, DNA replication and nuclear support [9]. Even though the A- and B- type lamins work interactively to maintain structural integrity of the nuclear lamina, they still have independent functions and varying gene expression patterns. A-type lamins, lamin A and C, are developmentally regulated proteins primarily expressed in most differentiated cells. Aside from their structural role, these lamins are found to be localized in the nucleoplasm near sites of RNA processing and DNA synthesis suggesting their involvement in processes like gene expression and DNA replication [9]. The B-type lamin proteins are expressed largely during the stages of development and cellular differentiation. *Lmnb1* knockout embryos showed multiple abnormalities in different areas of the brain with abnormal layering of neurons in the cerebral cortex, reduced number of neurons overall and multiple defects in the cerebellum and hippocampus [10]. While many studies have since been conducted to further analyze this gene duplication, the exact mechanisms by which this overexpression results in ADLD is, for now, uncertain.

Further investigations to decode the molecular mechanism involved in ADLD disease progression led to the creation of oligodendrocyte specific transgenic mice models overexpressing the LMNB1 protein. Findings indicated that oligodendrocyte specific *Lmnb1* overexpression was sufficient to induce molecular and pathological defects similar to those found in ADLD patients. These mice exhibited significant myelin sheath abnormalities along with axonal disintegration, a significantly higher myelin-axon unit degradation cohort, cognitive and memory impairments and progressive motor impairment when compared to the wild type controls [11]. Building on this previous research another study also based on oligodendrocyte specific transgenic mice, identified significant lipid dysregulation. Based on their findings, the researchers hypothesize that lipid dysregulation may have a critical contribution that leads to the demyelination phenotype and other

3

secondary pathologies like inflammation that exacerbate myelin sheath injury ultimately leading to neuronal cell death and axonal damage [12]. Further research studies will allow more definitive mechanisms to come forward, adding to our present knowledge and also confirming current findings.

1.3 Knock Out Mouse Models and ADLD

Research using total *Lmnb1* knockouts have been insightful in further understanding the role of this protein in development. Studies that generated total *Lmnb1* knockouts showed postnatal lethality due to respiratory failure, decreased body sizes and microcephaly compared to a normal control group [13]. *Lmnb1* knockout mice generated by another group exhibited perinatal lethality and multiple abnormalities in the skeletal structure, lungs and brain [14].

To understand the role of proteins that result in lethality when knocked out embryonically, conditional knockouts may be generated whereby the ablation of these proteins can be regulated in a cell specific and temporal manner. The Cre-*Lox*P system is a valuable tool used by researchers to generate these conditional knockouts models, both tissue/organ specific and inducible knockouts [15]. The general mechanism of the Cre-*Lox*P system involves the flanking of the gene of interest with *Lox*P sites, which is then recognized by a single Cre-recombinase and subsequently excised [16]. Using this methodology allows for researchers to have a more stage-specific and tissue-specific control over gene expression. For inducible knockouts tamoxifen is needed and it allows downstream processing leading to the knockout. In this system, a modified Cre protein is generated, via fusion with the Estrogen Receptor (ER) containing a mutated ligand domain. In the presence of tamoxifen, the Cre-ER bound protein undergoes nuclear translocation [16]. Through

this mechanism Cre recombinase can recognize the *Lox*P sites flanking gene of interest producing the required knockout via excision of the DNA segment between the *Lox*P sites.

Conditional *Lmnb1* knockout in forebrain (fb) specific neurons resulted in neuronal migration defects, an overall smaller number of neurons and significantly small cerebral cortices [10]. This study helped prove that LMNB1 protein reduction was enough to cause severe neurodevelopmental abnormalities resulting in a significantly smaller forebrain **(figure 2).** However, it is important to remember that in this case the knockout of *Lmnb1* also occurred during embryonic development albeit only in forebrain neurons.
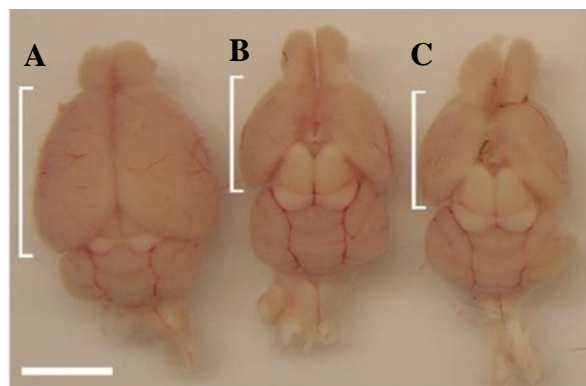
Figure 2: Forebrain-specific deletion of Lamin b1

Figure 2: shows the effect of forebrain-specific laminb1 deletion has on the overall size and morphology of the brain [10]. (A) normal brain without *Lmnb1* deletion (B) and (C) significantly small forebrain because of fb-specific knockout.

1.4 Public Health Significance

ADLD is a rare disease which currently does not have any treatment. This presents a vital clinical need for research and further investigation. Based on previous studies it has been

confirmed that ADLD in humans is caused by a *LMNB1* duplication and resultant overexpression [5]. Research at the Padiath lab is focusing on reducing expression levels of *LMNB1* in adulthood as a potential therapeutic strategy for ADLD. Based on previous studies in mice it is well known that *Lmnb1* ablation results in lethality during development. However currently, it is unclear whether reducing Lmnb1 levels specifically in adulthood would have any detrimental effect. Understanding this would be an important consideration for the future development of any ADLD therapy based on reducing *Lmnb1* expression. My project is significant as we will explore the effects of *Lmnb1* reduction during adulthood, in mice, as a precursor to developing therapies for ADLD.

1.5 Specific Aims and Project Description

Characterize and study a conditional knockout mouse model where *Lmnb1* is ablated ubiquitously during adulthood using the Cre-*Lox*P system.

Aim 1: Generation and characterization of mice where *Lmnb1* has been ablated ubiquitously in all tissues during adulthood. *Lmnb1* floxed (*Lmnb1* fl/fl) mice will be crossed to transgenic mice where Cre is ubiquitously expressed upon the administration of tamoxifen. The UBC Cre ERT; *Lmnb1* fl/fl mice (cKO) will be injected with tamoxifen at 2 months old to ablate *Lmnb1*1 expression. A *Lmnb1* fl/fl cohort (Ctrl) will also be generated and simultaneously injected with tamoxifen to produce the most suitable controls for the course of our study. We will confirm that *Lmnb1* is reduced at both the protein and RNA levels in a variety of different tissues.

Aim 2: Study the effect of *Lmnb1* ablation on behavior and histopathology of our cohort. We will identify whether knockout of *Lmnb1* during adulthood has any obvious phenotypic effects that result in abnormalities.

For the behavioral analysis of the cohort, rotarod and open field tests would be conducted. For the rotarod the mice are trained to run on a rod and the time at which they fall off the rod is recorded. For open-field analysis mice are individually allowed to explore the open-field chambers and multiple motor parameters are recorded using infrared detectors. These tests will serve a dual purpose and will allow us to understand their cognitive capabilities (with the training) and also their motor function which would be measured by their ability to run on the rod and how long they can run/ stay on the rod for. This paired with an assessment of exploratory and locomotor activity during the open-field test will provide us with the means to perform a comprehensive qualitative analysis. In cases where limb functionality is compromised it would be difficult for the mice to produce similar results to the Ctrl cohort allowing us to draw definitive conclusions. Since the germline knockouts exhibit significant CNS abnormalities, studying cognitive and motor function in the adult ablated *Lmnb1* mice is a logical approach. We will also carry out gross morphological and histopathological analysis of the brain and spinal cord from the LMNB1 ablated mice.

2.0 Materials and Methods:

2.1 Generation and breeding of the mice

Two groups of mice were needed for the course of this study: conditional knockouts (cKO) and control group (Ctrl). The UBC Cre ERT (Jackson Laboratories stock No.008085) mice were mated to homozygous *Lmnb1* fl/fl [10], (Jackson Laboratories stock No. 032558) mice to produce UBC Cre ERT; Lmnb1 fl/+. These UBC Cre ERT; Lmnb1 fl/+ were then crossed to *Lmnb1*fl/fl (Ctrl) in order to produce 25% of our conditional knockout (ckO) with the genotype UBC Cre ERT; *Lmnb1* fl/fl mice and 25% Lmnb1 fl/fl (Ctrl). Other possible genotypes produced were 25% *Lmnb1* fl/+ and 25% UBC Cre ERT; *Lmnb1* fl/+ (**figure 6A).**

Tamoxifen injections were administered intraperitoneally (IP) to both the control group and cKO mice. The mice were between 3-4 months old when the 1_{st} injections were administered. Tamoxifen (Sigma) was dissolved in corn oil (Sigma) at 20 mg/ml and administered at 75mg/kg body weight for 5 consecutive days on 3 separate occasions. 2-week breaks were administered between injection days to minimize stress on the cohort **(figure 3).** Rotarod was conducted 4 months post 1_{st} tamoxifen injection and open field was conducted 6 months post 1_{st} injection, due to some logistical reasons we were unable to conduct both tests within the same month. Mice were euthanized followed by harvested for tissue, 5 months post 1_{st} injection of Tamoxifen when the mice were between 7 and 9 months old.

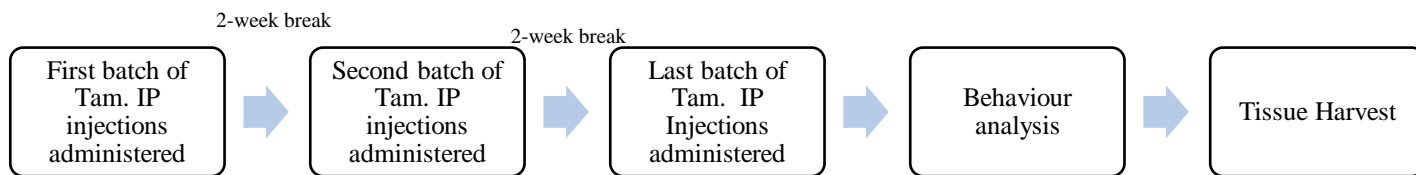| First batch of Tam. IP injections administered | → | Second batch of Tam. IP injections administered | → | Last batch of Tam. IP Injections administered | → | Behaviour analysis | → | Tissue Harvest |

Figure 3: Tamoxifen IP injections and project schematic

Figure 3: Schematic of our tamoxifen injections and overall materials and methods. Injections were administered over a 2-month time period, at 3 separate occasions with 2 week breaks in between to ensure no extra stress on the mouse cohort. Followed by behavior analysis tests and tissue harvest procedures.

2.2 Rotarod Behavior Analysis

To assess motor coordination and motor skill learning, the rotarod behavior analysis test was performed at the Rodent Behavior Analysis Core (RBAC) University of Pittsburgh based on Preclinical Phenotyping Core (PPC) approved protocols. Briefly, the test began with an hour-long habituation. With a sample size of n=11Ctrl and n=10 cKO, the mice were gently placed on the rotating cylindrical rod such that they interfered with the infrared beam **(figure 4).** The rod accelerates from 0 to 30 rotations per minute (RPM), increasing 0.2 revolutions per 1 second (150 seconds total) and stops at a final speed of 40 RPM. The rod rotates for a total set time of 300 seconds (s) and the exact point at which the mouse falls off the rod and hence, is no longer in contact with the infrared beam, is recorded. The parameters tested were latency average, body weight, latency trails by genotypes and strain. Statistical analysis was conducted using Graph Pad Prism software and comparison between the Ctrl and cKO cohort was drawn.
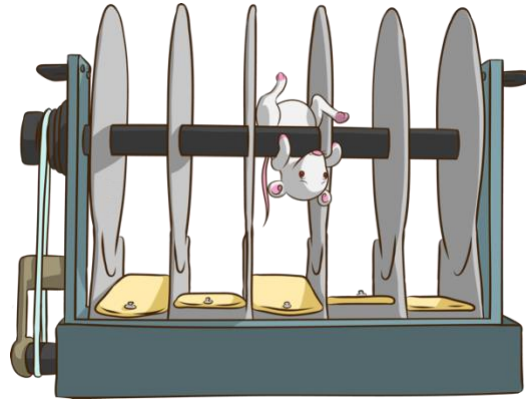
Figure 4: Rotarod apparatus

Figure 4: Illustration representative of the rotarod equipment used to conduct the behavior analysis test. Each mouse is placed on the rod, separated by dividers. The total time they remain running while the rod rotates is recorded once the mice fall off.

2.3 Open field activity monitoring test

Open field was performed at the RBAC at the University of Pittsburgh in a controlled environment, based on PPC approved protocols. We worked with a sample size of n=8 for each group (i.e. Ctrl and cKO), with ages ranging from 8 months to 10 months at the time of the analysis. Mice were individually placed into an open-field chamber (43 x 43 x 30 cm; Med Associates) **(figure 5)** and were allowed to explore for 60 minutes while data was collected. Infrared beams and monitors within the chambers allowed all our parameters of interest to be measured: Margin time, vertical time, total distance travelled, ambulatory time. A comparison was drawn between the Ctrl and cKO mice and the data was analyzed using Excel and Graph Pad Prism software.
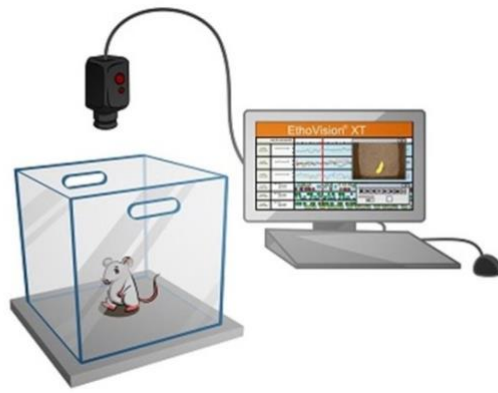
Figure 5: Open field apparatus

Figure 5: Illustration representative of the Open field behavior analysis test conducted. Each individual mouse is placed in a chamber, as shown, and is allowed to freely explore the area. Infrared beams sensors record every movement and produce data that is then analyzed.

2.4 Tissue Harvest and Processing

The mice were euthanized using the CO_2 chamber according to approved protocols, weighed and then harvested for tissue. For the purpose of our study we collected forebrain, spinal cord, heart and liver tissue. All samples were temporarily stored in liquid nitrogen followed by storage at -80°C until ready for further processing. The tissue samples were used for the isolation of genomic DNA, RNA and protein**.**

A standard genotyping PCR was conducted using gDNA extracted from a forebrain sample, via the Gentra Puregene Tissue Kit (Qiagen) according to the manufacturer's instructions. Using standard PCR protocols, lamin b1 allele in Ctrl cohort was identified by amplifying 2 regions of 1.5kb and 643 bp product as a means to cross verify the genotypes (**figure 6B).** The same primers generated a PCR fragment of 348 bp in the cKO mice **(figure 6C).** Genotyping primers and sequences are detailed in **table 3.**

2.5 RNA extraction and real time PCR

Samples were processed for RNA isolation in TRIzol (Invitrogen) using a motorized homogenizer (Kimble) and extracted based on the manufacturer's protocols. cDNA was synthesized from 1µg of RNA, from the previous step, using Qscript (Quanta Bio). Real-time PCR was conducted using SYBR Green SuperMix (Quanta Bio) and the experiment was run on an ABI Quant Studio 12K Flex (Biosystems). Data was analyzed using the $\Delta\Delta CT$ method [17] using the following primers: Ms. Lb1 to detect laminb1 expression levels and β-Actin (*Actb)* as the endogenous control. Real-time PCR primer sequences are in **table 4.**

2.6 Western Blot Analysis

Cellular protein (35-40 µg) was extracted using 1x proteinase inhibitor and T-PER cocktail solution (Thermo Scientific). Protein concentration was measured using the BCA protein assay kit (Thermo Scientific). The analysis was performed with dilutions of 35-40 µg of protein for each individual sample. Protein samples were run on a 10% Acrylamide gel (Bio-Rad) and then transferred to nitrocellulose membrane (Bio-Rad) for detection. The blocking step involved the use of 3% non-fat dry milk, made using 1X TBS and powdered milk, set on a gentle shaker for 1 hour at room temperature. The membranes were incubated over night with primary antibodies diluted in 1x Odessy blocking buffer with 0.1% Tween-20 (Fisher) at 4°C with gentle shaking. Primary antibodies used and their dilutions are listed in **table 1**. The next morning, membranes were washed thrice, for 10 minutes each, with TBS-T (TBS +0.1%Tween 20), and further incubated with secondary antibodies in Odessy blocking buffer and 0.1% Tween 20 for 1 hour at

12

room temperature in black boxes to reduces any light exposure. After a repetition of the washing step the membranes were scanned, analyzed and quantified using the LI-COR Odyssey CLx infrared scanner and Image Studio software (LI-COR Biosciences). Secondary antibody details are listed in **table 2**.

2.7 Cell culture and Immunohistochemistry

Ear fibroblast cells were cultured from ear tissue obtained from 10-month-old Ctrl and cKO mice, both had been injected with tamoxifen. The ear punches were ground and incubated with dispase II 1 mg/mL in DMEMF-12 (Millipore #SCM133) and collagenase II 1 mg/mL in DMEMF-12 (MPBio #100502) for 2 hours at 37 °C with gentle mixing every 20-30 minutes. The pieces were then washed with DMEM (high glucose DMEM (Corning) supplemented with 10% FBS (Fisher) and centrifuged to produce a pellet and discard the supernatant. After a few washes we resuspend the pellet in DMEME complete (high glucose DMEM (Corning) supplemented with 10% FBS (Fisher), 2mM L-glutamine (Millipore), and 1% Penicillin streptomycin (Hyclone)) before proceeding to plate in 6-well dish to allow cells to proliferate and be passaged as usual. The cells were added onto glass coverslips and incubated at 37 °C until they reached the desired confluency of 70-90%. To fix the cells we began with washing them with 1X DPBS (Sigma), followed by 4% formaldehyde (Ted Pella) in PBS for 15 minutes at room temperature. After washing with PBS, blocking and permeabilization was performed simultaneously, for 1 hour at room temperature, using the blocking buffer:1X PBS +5% normal donkey serum (Jackson ImmunoResearch) +0.3% Triton X-100 (Sigma). Primary antibodies were diluted using the above described blocking buffer and incubated with cells overnight at 4°C. Primary antibodies used and

their dilutions are listed in **table 1**. The next day, primary antibody dilutions were discarded, and cells were washed with PBS thrice for 5 minutes each at room temperature. Next step involved the use of secondary antibodies, FITC and Cy3 as listed in **table 2**, each diluted with 1:350 PBS and incubated with the cells at room temperature in the dark for 1 hour. Cells were washed thrice again with PBS before being mounted onto glass microscope slides using vectashield antifade mounting medium with DAPI (Vector Laboratories). The images were taken with Leica DM5000B upright microscope with a 40x lens magnification and a Leica DFC310 FX digital camera.
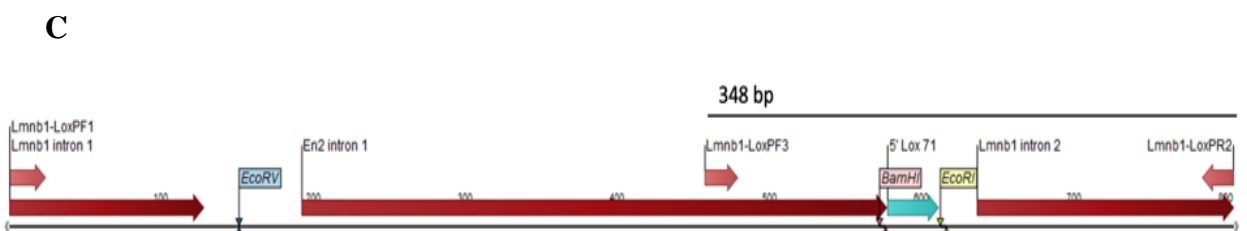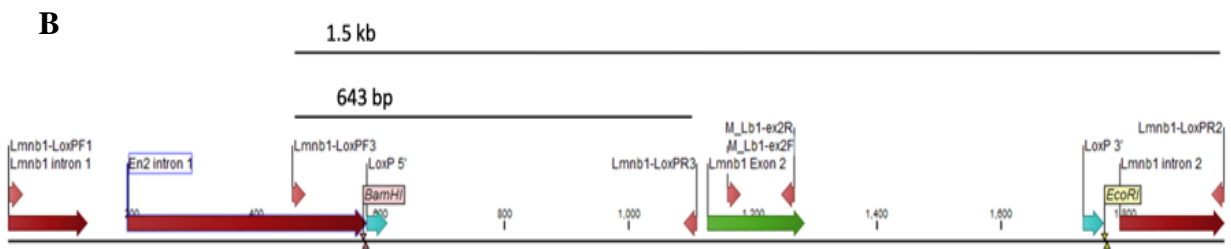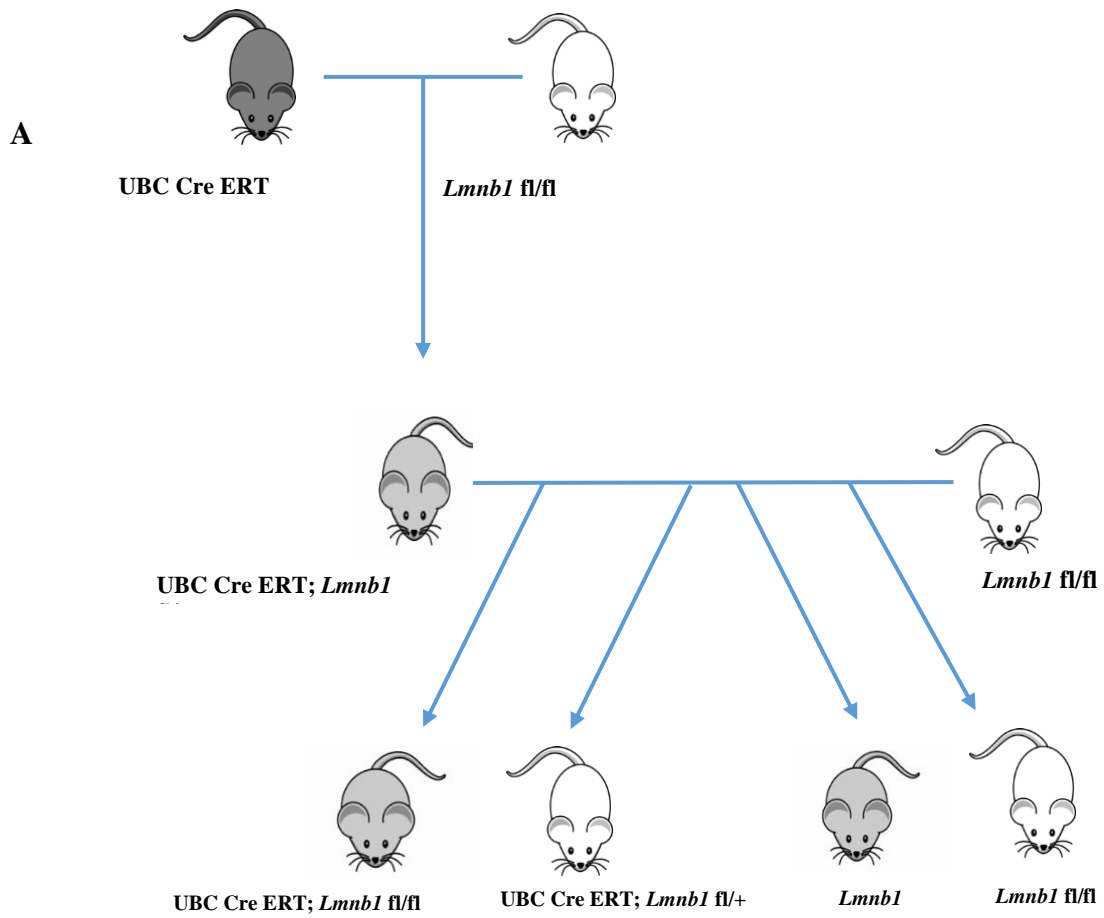
2.8 Weight Analysis

A bi-weekly weight in (g) was recorded for a total of 30 weeks, in order to analyze any weight changes that might be significantly different between the Ctrl and the cKO mice. The statistical analysis was done using Graph Pad Prism software.

3.0 Results

3.1 Reduced *Lmnb1* expression found in cKO mice

UBC Cre ERT; *Lmnb1* fl/+ mice were crossed to *Lmnb1* fl/fl mice to produce offspring with the desired genotype for our cKO mice i.e. UBC Cre ERT; *Lmnb1* fl/fl (**figure 6A**). To confirm the genotypes of mice and to confirm that tamoxifen administration ablated the Lmnb1 gene we used genotyping PCR primers designed to amplify specific regions in control and cKO mice **(figure 6B and 6C).** Amplification of Ctrl samples results in the production of 2 fragments each, 1.5kb and 643 bp, compared to 1 fragment of 348 bp in samples from cKO mice. In **figure 6D** the PCR shows results obtained using genomic DNA extracted from forebrain samples and the positive controls used are previously confirmed Ctrl and cKO samples. This genotyping experiment confirmed that *Lmnb1* had been successfully knocked out in the cKO mice while still intact in our Ctrl cohort, preparing us for the following molecular analysis techniques. We expected to see a reduction in LMNB1 levels only in the conditional knockout mice cohort.

A

UBC Cre ERT

Lmnb1 fl/fl

UBC Cre ERT; *Lmnb1*

Lmnb1 fl/fl

UBC Cre ERT; *Lmnb1* fl/fl   UBC Cre ERT; *Lmnb1* fl/+   *Lmnb1*   *Lmnb1* fl/fl

B

1.5 kb

643 bp

Lmnb1-LoxPF1
Lmnb1 intron 1   En2 intron 1   Lmnb1-LoxPF3   LoxP 5'   BamHI   Lmnb1-LoxPR3   Lmnb1 Exon 2   M_Lb1-ex2R   M_Lb1-ex2F   LoxP 3'   EcoRI   Lmnb1-LoxPR2   Lmnb1 intron 2

C

348 bp

Lmnb1-LoxPF1
Lmnb1 intron 1   EcoRV   En2 intron 1   Lmnb1-LoxPF3   5' Lox 71   BamHI   EcoRI   Lmnb1 intron 2   Lmnb1-LoxPR2
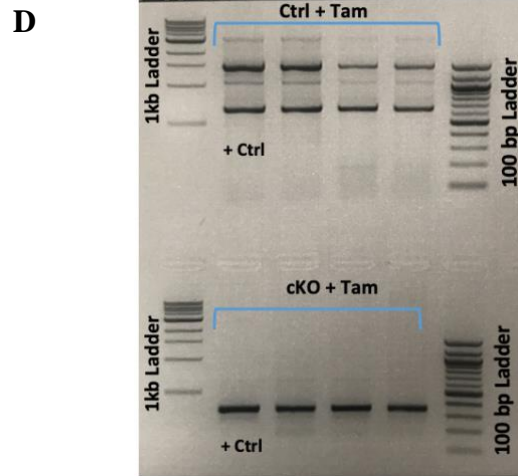
Figure 6: Generation of mice and genotyping

Figure 6: (A) Schematic of how the cKO mice i.e.UBC Cre ERT; *Lmnb1* fl/fl mouse were produced and all possible genotypes (B) shows the fragments produced in Ctrl by primers LoxPF3, LoxPR2, LoxPR3 (C) shows the fragment amplified in cKO mice samples. Figure C shows the PCR results using previously described primers. The controls used are positive controls for both Ctrl and cKO and the gel is run with ladders on each end of the gel. (D) gel results of genotyping PCR showing 2 bands produced after amplification in the Ctrl samples as described above and only 1 band in the cKO knockout mice as a result of the tamoxifen induced knockout.

IHC performed using ear fibroblast cells from Ctrl (**figure 7A**) and cKO **(figure 7B)** respectively showed a reduced percentage of lamin b1 expression in the knockout mice. Cells were counted from 5 different fields within the same slide. Assessment of the data obtained by IHC established that only 37.9% of the total number of cKO cells expressed Lmnb1 protein when compared to the Ctrl **(figure 7C).** A t-test performed allowed us to calculate a p value of 0.0079, with $p < 0.05$ considered significant, showing how the difference in LMNB1 expression seen in the Ctrl and cKO cells is statistically significant.

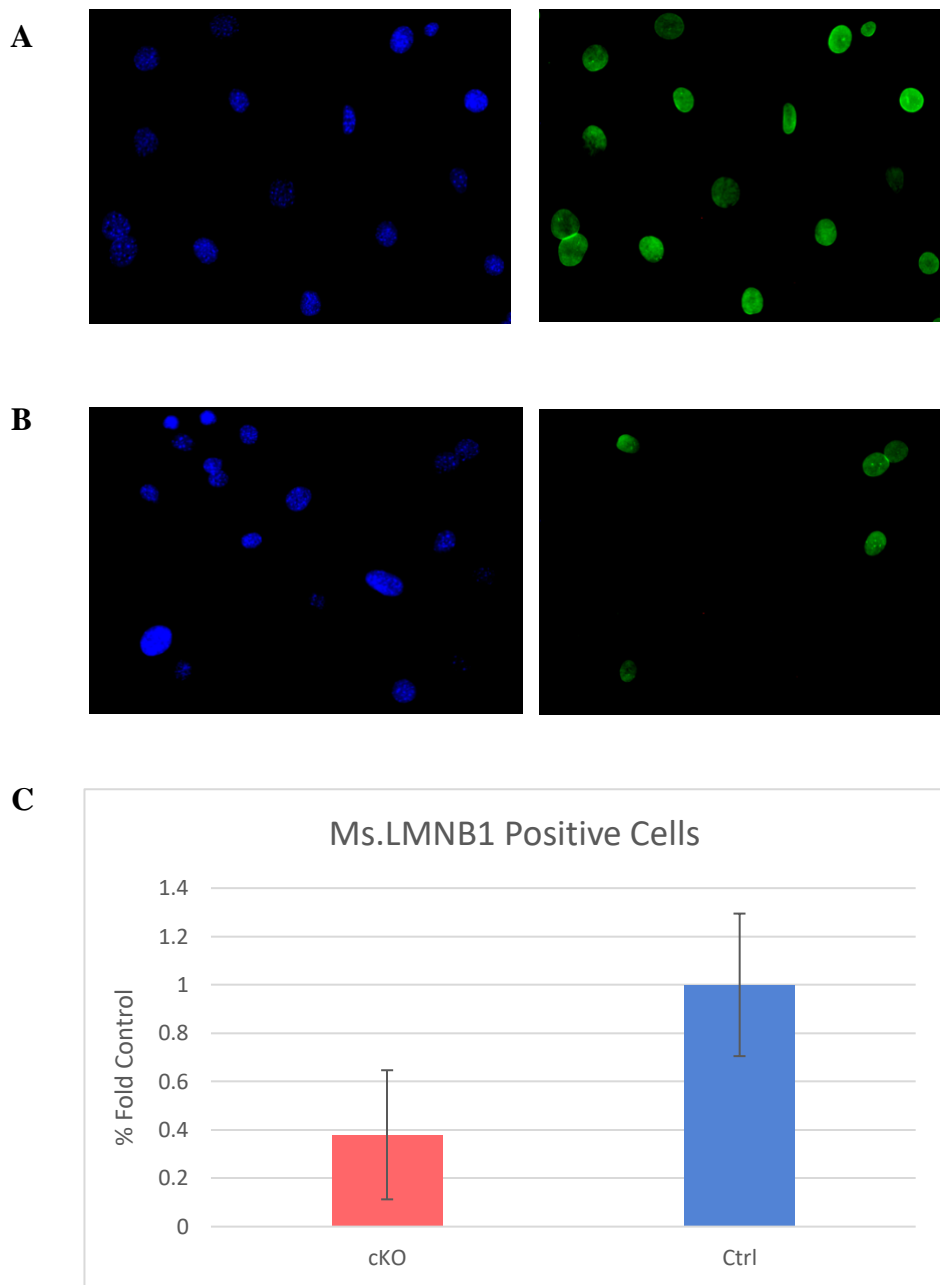**Figure 7: Immunohistochemistry imaging and quantification**

Figure 7: (A) Ctrl ear fibroblasts cells stained with DAPI (blue), Lmnb1 (green). A normal amount of LMNB1 stained cells are seen. (B) cKO ear fibroblasts cells stained with DAPI (blue), Lmnb1 (green). A reduced number of Lb1 stained cells are seen. (C) Bar graph shows the % expression of Lb1 positive cells in ckO and Ctrl groups with a p-value=0.007.

Real-time PCR and immunoblot analysis used RNA and protein lysates obtained from forebrain, spinal cord, heart and liver for each individual mouse. The sample size for this analysis was n=3 for each cohort. Tissue samples isolated; i.e. forebrain, spinal cord, heart and liver, from each individual mouse were obtained and treated independently. Results are shown in **figure 8**. In the real time PCR results, all cKO samples show a significant reduction in *Lmnb1* expression across all tissues **(figure 8A**). Statistical analysis test, using the Ctrl samples as controls, rendered significant p values as shown in **figure 8A**. Protein expression patterns reported in our immunoblot were more variable with significant p values in the forebrain and spinal cord only **(figure 8B).** A t-test was used to analyze the statistical significance in both our RNA and protein expression data. An immunoblot representative image is also shown **(figure 8C).** Older data carried out by another lab member, however, is consistent with a significant reduction in LMNB1 protein expression **(figure 8D).** This discrepancy maybe due to technical issues, or alternatively due to a difference in the knockout percentage. Our aim was to repeat our western blot in order to produce the most reliable and accurate result however we were unable to do that because of the labs being closed down temporarily owing to the coronavirus pandemic.
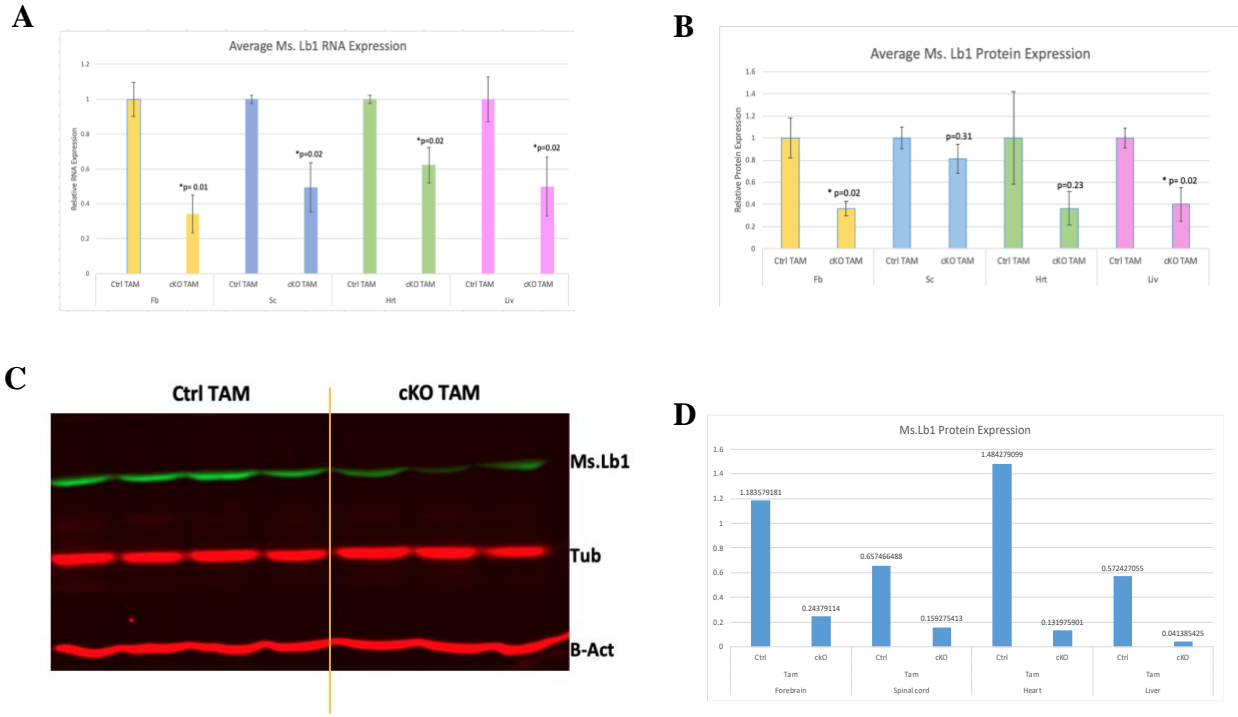
Figure 8: Real-time PCR data and immunoblot analysis

Figure 8: (A)Real-time PCR data showing the average mouse *Lmnb1* RNA expression, significant p-values are reported with fb rendering p=0.01 and the p=0.02 in the other tissues. (B) Immunoblot data showing the average laminb1 protein expression pattern obtained, significance is reported in Fb and Liv only with p values <0.05, differences seen in Sc and Hrt are not significant. (C) Western blot of liver protein lysates run on an acrylamide gel obtained from 4 Ctrl and 3 cKO mice. (D) Protein expression obtained in previously run data to show the drastic reduction in expression (n=1 Ctrl and n=1 cKO).

3.2 No recognizable differences in brain development and overall weight

A cursory comparison of the whole brain between the Ctrl and cKO did not show any substantial differences in brain size or gross morphology **(figure 9A).** This was important to establish because previous studies show embryonic *Lmnb1* knockout is responsible for

neurodevelopmental abnormalities leading to the underdevelopment of the brain, as described earlier [10] *(figure 2).* Here we are able to demonstrate how *Lmnb1* reduction, to 30-40 % levels, in adulthood has no such effects as the brains of both Ctrl and cKO mice look grossly similar. We were also planning to carry out immunohistochemical analysis of the brain tissue from the two groups of mice to determine whether there were any abnormalities in the cellular organization of key structures of the CNS such are the cortex and cerebellum that were shown to be disrupted in the global *Lmnb1* knockouts. However, our plans were disrupted by the coronavirus outbreak.

Throughout the course of the study, until the mice were harvested, their weight in grams (g) was recorded bi-weekly to observe any gain or loss and to identify if any significant differences in weight could be observed. A bi-weekly analysis was done (**figure 9B**), it included data from a total of 13 mice including both males and females, spanning 30 weeks in total. The beginning and end weights **(figure 9C)** were also separately quantified to see which group experienced more changes in weight and whether it was significant. The unpaired t-test found no significance with p values of 0.28 and 0.91 respectively. An overall percentage change in weight, using the beginning and the end weights, was analyzed using ordinary one-way ANOVA and a p-value of > 0.05 showed no significant differences.
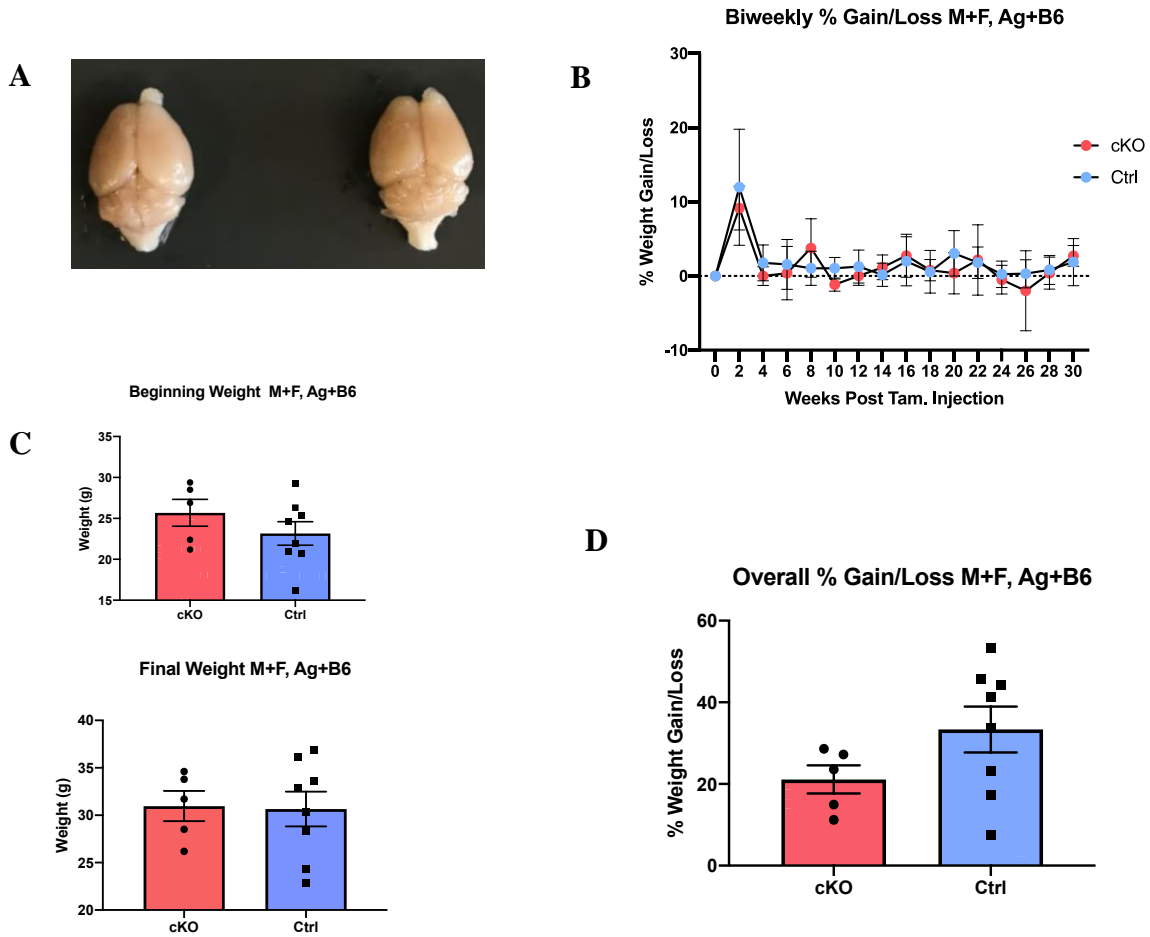
Figure 9: Brain morphology and weight analysis

Figure 9: No significant differences observed between the brains and the weight data. (A) Two perfused, para-formaldehyde fixed mouse brains placed side by side for comparison. Ctrl. (left) and cKO (right) do not exhibit any obvious differences in size, or gross morphology. (B) Biweekly % gain/loss analysis including all males and females over a period of 30 weeks, consisting of a total of 13 mice. (C) Comparison of beginning weights and final weights between cKO and Ctrl, p-value =0.28 for beginning weight and p-value =0.91 for final weight. (D) Overall % change in weight using the beginning and end weights, the difference seen is not significant with a p-value of 0.13

3.3 No differences in behavioral activity in cKO and Ctrl mice

The behavior analysis portion of our study included the rotarod test and the open field. Data collected and analyzed form both these methods showed no significant differences in the parameters measured **(figure 10A and 10B).** This led us to conclude that no significant phenotypic differences existed between the two groups. Using an unpaired t test to analyze the latency average we were able to calculate a p value > 0.05 and conclude that the result was not statistically significant.
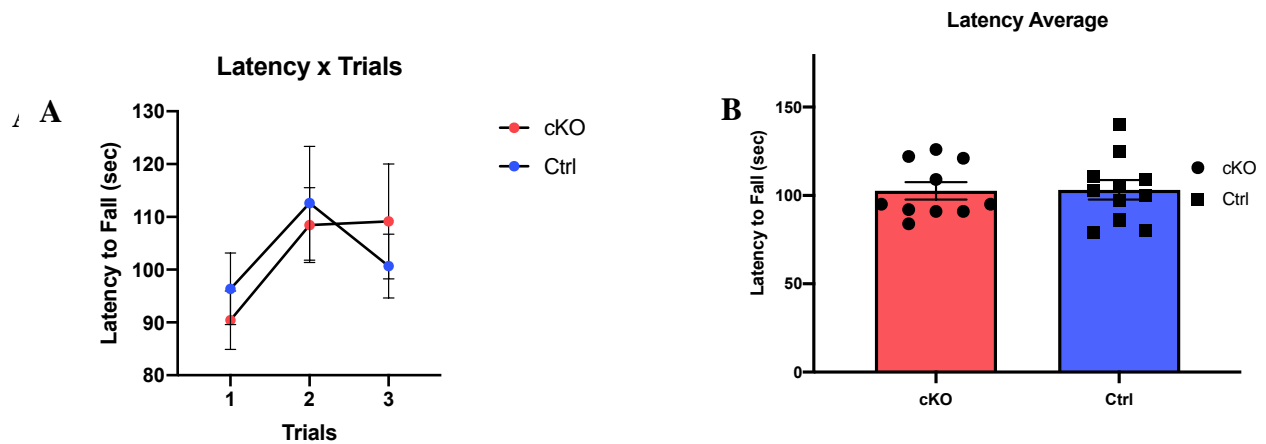

Figure 10: Rotarod data analysis

Figure 10: Sample size n=11 (Ctrl) and n=10 (cKO). No significant differences between cKO and Ctrl mice. (A) shows the latency to fall for all 3 trials conducted for cKO and Ctrl. (B) Latency average showing the average time mice from each cohort stayed on the rotarod. Difference between both groups was not significant with a p-value =0.93

The open field analysis allowed us to further investigate if any deleterious effects had been produced as a result of knocking out *Lmnb1*. We measured different parameters i.e. margin time, total distance, vertical activity, rest time movement time etc (**figure11).** Statistical analysis included the use of 2way ANOVA tests for all our parameters except ambulatory episode average velocity, ambulatory episode peak velocity and ambulatory episode median velocity. For those last parameters we used an unpaired t-test for statistical analysis. After our analysis we were able to conclude how each parameter showed no significant difference between the control and cKO groups based on our p-values which were all > 0.05, consistent with our findings in the rotarod test.
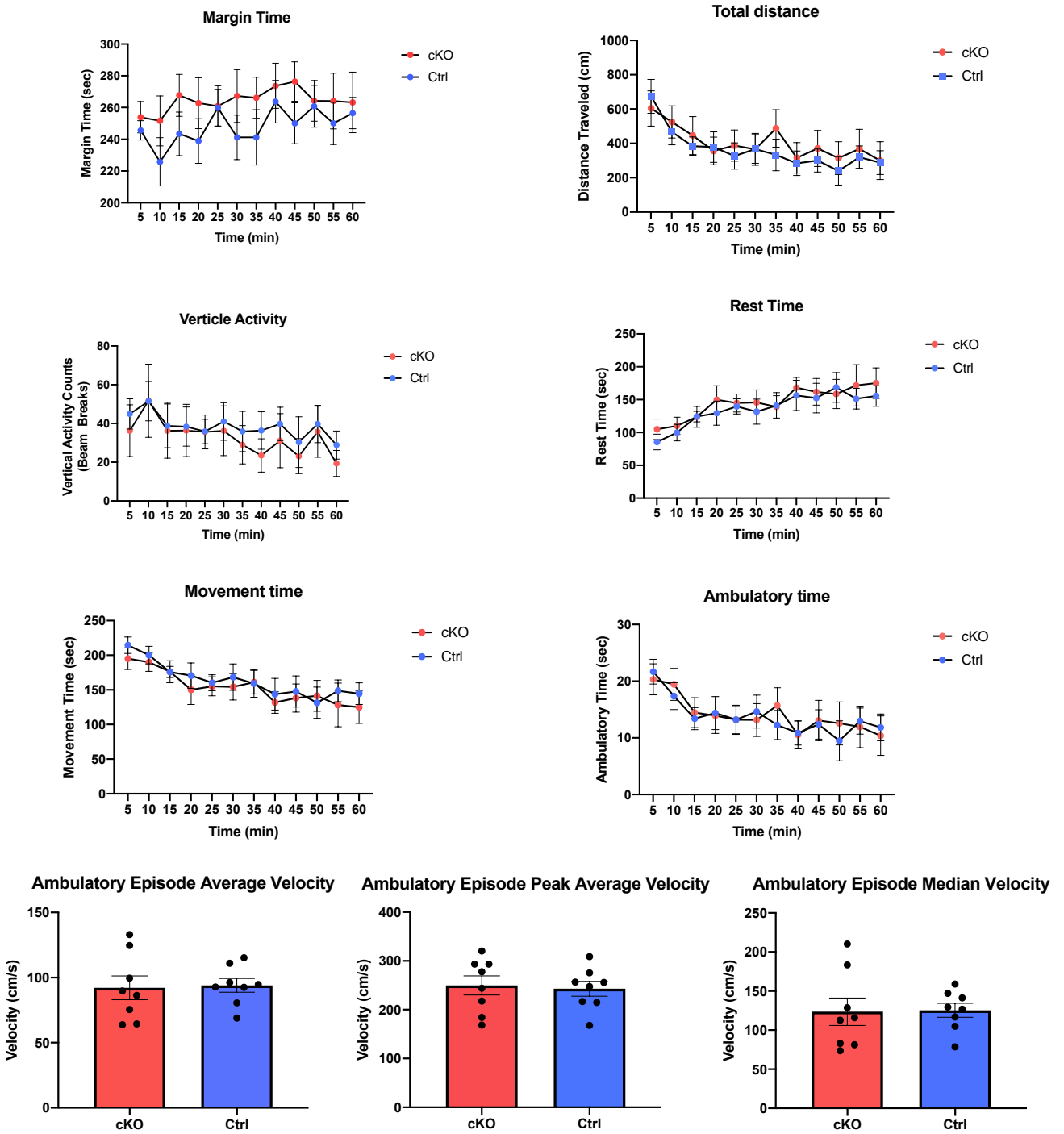
Figure 11: Open field data analysis

Figure 11: Sample size n=8 for each cohort (Ctrl and cKO). Data obtained from open field analysis shows no significant differences between cKO and Ctrl mice. All parameters measured and

quantified are shown in the diagrams in the figure above, and although variations existed none of the differences were significant with all p-values > 0.05.

4.0 Discussion

As previously discussed, ADLD is a rare condition that manifests in adulthood with an autosomal dominant inheritance pattern. The fact that no effective treatment exists poses an important public health problem. With research work now focusing on potential therapies to reduce *LMNB1* overexpression during adulthood, our project directly examines if *Lmnb1* reduction during adulthood, in mice, produces any deleterious effects.

In the current study we establish how *Lmnb1* knocked out, to 30-40%, in adulthood does not have any significant detrimental effects on behavior, activity and overall normal physical functionality. The mice used were closely monitored in the mouse facility throughout the duration of the study, and the control (Ctrl) and conditional knockout (cKO) mice were physically indistinguishable. They showed no signs and symptoms characteristic of ADLD like forelimb paralysis or difficulty in movement, eating and drinking etc. The results of the behavior analysis tests also remained consistent with this observation and there was no significant difference in activity recorded between both our study groups. Using genotyping techniques, we confirmed that the gene ablation had successfully taken place in our knockout mice, to 30-40% levels, while the control group retained normal *Lmnb1* functionality. With our molecular data we further studied the changes in RNA and protein expression patterns in different tissues i.e. forebrain, spinal cord, heart and liver. Analyzing these expression patterns gave us an understanding of the changes produced in all tissues after the knockout was induced.

It is important to point out that the assays that we have used rule out only gross morphological and behavioral alterations and more subtle abnormalities could still exist. A more detailed histological and molecular examination of various tissues is warranted to conclude that

LMNB1 loss during adulthood has no deleterious effects. It is also important to note the significant role LMNB1 plays in proliferation and its relation to the residual levels of gene and protein expression observed in our molecular analysis. In our cKO cohort we observe a residual expression of the protein, one major reason for this could be the possible proliferation and growth of cells that still contain LMNB1, while cells that no longer express *Lmnb1* will not proliferate and hence be seen in smaller numbers.

Studies conducted on other genetic conditions like Huntington's disease have also reported similar occurrences. Ablation of the target gene, *Htt*, in embryonic mouse models and even young mice results in postnatal death due to secondary pathologies however reducing the same target gene i.e. *Htt* in adulthood is reportedly non-deleterious [18]. This suggests that although these genes are vital for normal development, they may no longer be critical during adulthood.

As a result of our study, we conclude that ablation of *Lmnb1* levels to 30-40%, in adulthood produces no significantly deleterious effects. This suggests that reducing *LMNB1* levels during adulthood, at least to no more than 30-40%, is a potentially viable therapeutic strategy that might not produce any deleterious side effects and hence should be studied further. Since our results show 30-40% Lmnb1 activity remaining, after the knockout was administered, it would also be worthwhile for future studies to focus on identifying whether there is a lower threshold level below which phenotypic manifestations might occur.

Appendix: Tables

Table 1: Table of primary antibodies

Primary Antibody	Source	Company	Catalog #	WB Dilution	IHC Dilution
Anti-Lamin B1	Rabbit	Abcam	ab16048	1:4000	1:500
Anti-Beta-Actin Loading control	Mouse	Invitrogen	MA5-15739	1:5000	
Anti- Beta IV Tubulin- Loading Control	Rat	Abcam	ab179509	1:1000	
Anti- GAPDH	Mouse	Thermo	MA5-15738	1:5000	

Table 2: Table of secondary antibodies

Secondary Antibody	Source	Company	Catalog #	WB Dilution #	IHC Dilution
Anti-Mouse IRDye 680LT	Goat	LI-COR Biosciences	926-68020	1:10000	
Anti-Rabbit IRDye 800CW	Donkey	LI-COR Biosciences	926-32213	1:10000	
Anti-Rat IRDye 680 LT	Goat	LI-COR Biosciences	925-68029	1:10000	
Anti-Rabbit FITC	Donkey	Jackson ImmunoResearch	711-095-152		1:350
Anti-Mouse Cy3	Donkey	Jackson ImmunoResearch	715-165-150		1:350

Table 3: Table of genotyping primer sequences

Genotyping primers	Sequence (5´-3´)	Product size (bp)
Lmnb1-LoxPR3	ACACAATCACAACCTTGCCTTG	Lb1-fl/fl= 2 bands of 1.5 kb and 653 bp
Lmnb1-LoxPR2	GGGGTCACATCAAATCACCTA	Lb1Δ= 1 band of 348 bp
Lmnb1 LoxPF3	GAGATGCCAGAGACTCAGTGAA	

Table 4: Table of real-time PCR primer sequences

Real-time PCR Primers	Sequence (5´-3´)
Mouse. *Laminb1*	GCTGCTCAATTATGCCAAGAAG
	GCCGCATCCTTAGAGTTTAGT
Mouse. *Actb*	CCACTGCCGCATCCTCTTCC
	CTCGTTGCCAATAGTGATGACCTG

Bibliography

1.   Simons, M., & Trajkovic, K. (2006). Neuron-glia communication in the control of oligodendrocyte function and myelin biogenesis. *J Cell Sci, 119*(Pt 21), 4381-4389. doi:10.1242/jcs.03242

2.   van der Knaap, M. S., & Bugiani, M. (2017). Leukodystrophies: a proposed classification system based on pathological changes and pathogenetic mechanisms. *Acta Neuropathologica, 134*(3), 351-382. doi:10.1007/s00401-017-1739-1

3.   Padiath, Q. S. (2019). Autosomal Dominant Leukodystrophy: A Disease of the Nuclear Lamina. *Frontiers in Cell and Developmental Biology, 7*(41). doi:10.3389/fcell.2019.00041

4.   Meijer, I. A., Simoes-Lopes, A. A., Laurent, S., Katz, T., St-Onge, J., Verlaan, D. J., . . . Rouleau, G. A. (2008). A novel duplication confirms the involvement of 5q23.2 in autosomal dominant leukodystrophy. *Arch Neurol, 65*(11), 1496-1501. doi:10.1001/archneur.65.11.1496

5.   Padiath, Q. S., Saigoh, K., Schiffmann, R., Asahara, H., Yamada, T., Koeppen, A., . . . Fu, Y.-H. (2006). Lamin B1 duplications cause autosomal dominant leukodystrophy. *Nature Genetics, 38*(10), 1114-1123. doi:10.1038/ng1872

6.   Brussino, A., Vaula, G., Cagnoli, C., Panza, E., Seri, M., Di Gregorio, E., . . . Brusco, A. (2010). A family with autosomal dominant leukodystrophy linked to 5q23.2-q23.3 without lamin B1 mutations. *Eur J Neurol, 17*(4), 541-549. doi:10.1111/j.1468-1331.2009.02844.x

7.   Nahhas, N., Sabet Rasekh, P., Vanderver, A., & Padiath, Q. (2016). Autosomal Dominant Leukodystrophy with Autonomic Disease. In M. P. Adam, H. H. Ardinger, R. A. Pagon, S. E. Wallace, L. J. H. Bean, K. Stephens, & A. Amemiya (Eds.), *GeneReviews(®)*. Seattle (WA): University of Washington, Seattle Copyright © 1993-2020, University of Washington, Seattle. GeneReviews is a registered trademark of the University of Washington, Seattle. All rights reserved.

8.   Schuster, J., Sundblom, J., Thuresson, A. C., Hassin-Baer, S., Klopstock, T., Dichgans, M., . . . Dahl, N. (2011). Genomic duplications mediate overexpression of lamin B1 in adult-onset autosomal dominant leukodystrophy (ADLD) with autonomic symptoms. *Neurogenetics, 12*(1), 65-72. doi:10.1007/s10048-010-0269-y

9.   Vergnes, L., Péterfy, M., Bergo, M. O., Young, S. G., & Reue, K. (2004). Lamin B1 is required for mouse development and nuclear integrity. *Proc Natl Acad Sci U S A, 101*(28), 10428-10433. doi:10.1073/pnas.0401424101

10.   Coffinier, C., Jung, H. J., Nobumori, C., Chang, S., Tu, Y., Barnes, R. H., 2nd, . . . Young, S. G. (2011). Deficiencies in lamin B1 and lamin B2 cause neurodevelopmental defects and distinct nuclear shape abnormalities in neurons. *Mol Biol Cell, 22*(23), 4683-4693. doi:10.1091/mbc.E11-06-0504

11.   Heng, M. Y., Lin, S. T., Verret, L., Huang, Y., Kamiya, S., Padiath, Q. S., . . . Fu, Y. H. (2013). Lamin B1 mediates cell-autonomous neuropathology in a leukodystrophy mouse model. *J Clin Invest, 123*(6), 2719-2729. doi:10.1172/jci66737

12.   Rolyan, H., Tyurina, Y. Y., Hernandez, M., Amoscato, A. A., Sparvero, L. J., Nmezi, B. C., . . . Padiath, Q. S. (2015). Defects of Lipid Synthesis Are Linked to the Age-Dependent

Demyelination Caused by Lamin B1 Overexpression. *The Journal of Neuroscience, 35*(34), 12002. doi:10.1523/JNEUROSCI.1668-15.2015

13.   Kim, Y., Sharov, A. A., McDole, K., Cheng, M., Hao, H., Fan, C. M., . . . Zheng, Y. (2011). Mouse B-type lamins are required for proper organogenesis but not by embryonic stem cells. *Science, 334*(6063), 1706-1710. doi:10.1126/science.1211222

14.   Yang, S. H., Jung, H. J., Coffinier, C., Fong, L. G., & Young, S. G. (2011). Are B-type lamins essential in all mammalian cells? *Nucleus, 2*(6), 562-569. doi:10.4161/nucl.2.6.18085

15.   Ray, M. K., Fagan, S. P., & Brunicardi, F. C. (2000). The Cre–loxP System: A Versatile Tool for Targeting Genes in a Cell- and Stage-Specific Manner. *Cell Transplantation, 9*(6), 805-815. doi:10.1177/096368970000900607

16.   Kim, H., Kim, M., Im, S. K., & Fang, S. (2018). Mouse Cre-LoxP system: general principles to determine tissue-specific roles of target genes. *Lab Anim Res, 34*(4), 147-159. doi:10.5625/lar.2018.34.4.147

17.   Livak, K. J., & Schmittgen, T. D. (2001). Analysis of relative gene expression data using real-time quantitative PCR and the 2(-Delta Delta C(T)) Method. *Methods, 25*(4), 402-408. doi:10.1006/meth.2001.1262

18.   Wang, G., Liu, X., Gaertig, M. A., Li, S., & Li, X. J. (2016). Ablation of huntingtin in adult neurons is nondeleterious but its depletion in young mice causes acute pancreatitis. *Proc Natl Acad Sci U S A, 113*(12), 3359-3364. doi:10.1073/pnas.1524575113